JOURNAL OF COMPUTATIONAL PHYSICS 76, 131–158 (1988)

# Time-Independent and Time-Dependent Potential Scattering without Angular Momentum Decomposition

J. HOLZ AND W. GLÖCKLE

*Theoretische Physik II, Ruhr-Universität Bochum, D-4630 Bochum 1, West Germany*

Received February 13, 1987

The Lippman–Schwinger equation for the $t$-matrix in three-dimensional space is solved directly without angular momentum decomposition As an alternative to avoid the propagator singularity we also study the time-dependent Schrodinger equation. It is solved in integral form and in momentum space by using complex momenta This damps the energy dependent time factors which for real momenta would be difficult to handle numerically Examples demonstrate feasibility and usefulness 

## I. INTRODUCTION

Angular momentum conservation for scattering on a scalar potential is a well-accepted simplification and reduces the scattering problem to a set of uncoupled one-dimensional equations. For higher energies, however, many partial waves may contribute to a scattering amplitude. Whereas the higher partial-wave amplitudes show a strong oscillatory angular behaviour, the full scattering amplitude often behaves rather smoothly and the decomposition into "violent pieces" should be avoided. We therefore study the direct solution of potential scattering in three-dimensional space without angular momentum decomposition. Since we work in momentum space this involves the direct solution of the Lippmann–Schwinger equation (LS) for the $T$-matrix depending on vector variables. This could have useful applications. In the two-nucleon problem, for instance, the forces are spin-dependent and the angular momentum decomposition is quite tedious. This can be avoided as we shall demonstrate in a forthcoming paper. Here we shall restrict ourselves to spinless particles. The way we solve the three-dimensional LS equation together with a numerical example is shown in Section II.

Solving a LS equation for potential scattering one faces the Cauchy singularity $(E+i\varepsilon-E')^{-1}$ which can be treated by standard techniques. For three particles, however, the free propagator singularity combined with a partial-wave decomposition yields quite unpleasant "moving" logarithmic singularities. Obviously, one avoids singularities completely in a time-dependent formulation. As our first step



0021-9991/88 $3 00

we therefore study the solution of time-dependent potential scattering in three-dimensional space without angular momentum decomposition. There are solutions of the time-dependent Schrödinger equation in one space-dimension and we are aware of three-body systems treated either in a collinear approximation or in an Euler angle decomposition. The strong oscillations occuring in configuration space [1, 2], however, led us quickly to regard a momentum space representation instead. We present two approaches. In the first one the evolution of the scattering state is followed from large negative times towards $t=0$ and the time evolution of auxiliary states from large positive times backwards to $t=0$. These auxiliary states develop out of a suitable chosen set of initial wavepackets. They have to be general enough such that by a linear combination one can represent the physical state at $t=0$. Equating the two states at $t=0$ one can determine the on-shell scattering amplitude.

In the second approach we tame time and energy dependent oscillations in the state by choosing complex momenta. The dependence of the state on real momenta can be determined in a second step by quadrature. Both approaches are described in Section III. We illustrate the first approach with a numerical example in one space-dimension. The second approach, which we favour, is examplified by a numerical example in three-dimensional space in Section IV. There we also describe how we handle the time dependence by a linear or cubic interpolation. A more sophisticated interpolation by cubic B-splines is described in the Appendix. We summarize in Section V.

## II. Stationary Potential Scattering

The LS equation for the half-shell $T$-matrix reads

$$T(\mathbf{q}, \mathbf{q}_0) = V(\mathbf{q}, \mathbf{q}_0) + \int d^3q' V(\mathbf{q}, \mathbf{q}') \frac{1}{E_{q_0} + i\varepsilon - E_{q'}} T(\mathbf{q}', \mathbf{q}_0) \qquad \left(E_{q_0} = \frac{\mathbf{q}_0^2}{2m}, E_{q'} = \frac{q'^2}{2m}\right) \tag{II.1}$$

Let us assume a scalar potential $V(\mathbf{q}, \mathbf{q}')$ which depends on $q \equiv |\mathbf{q}|$, $q' \equiv |\mathbf{q}'|$, and $y = \hat{q} \cdot \hat{q}'$. As a consequence $T$ depends on $q$, $q_0$ and $x = \hat{q} \cdot \hat{q}_0$. In explicit notation and dropping the $q_0$-dependence in $T$ we get

$$T(q, x) = V(q, q_0, x) + \int_0^\infty dq' q'^2 \int_{-1}^{+1} dx' \int_0^{2\pi} d\varphi' \times V(q, q', y) \frac{1}{E_{q_0} + i\varepsilon - E_{q'}} T(q', x'). \tag{II.2}$$

Obviously, we can put $y = xx' + \sqrt{1-x^2}\sqrt{1-x'^2}\cos\varphi'$ and recognize that the $\varphi'$-dependence occurs only in $V$. We introduce

$$v(q, q', x, x') = \int_0^{2\pi} d\varphi' V(q, q', xx' + \sqrt{1-x^2}\sqrt{1-x'^2}\cos\varphi') \tag{II.3}$$

and end up with a two-dimensional integral equation

$$T(q, x) = \frac{1}{2\pi} v(q, q_0, x, 1) + \int_0^{\infty} dq' q'^2 \times \int_{-1}^{+1} dx' v(q, q', x, x') \frac{1}{E_{q_0} + i\varepsilon - E_{q'}} T(q', x'). \tag{II.4}$$

This equation can be easily solved even on a modest computer. It may be advisable to introduce the real $K$-matrix through

$$K(q, x, x_0) = \frac{1}{2\pi} v(q, q_0, x, x_0) + \int_0^{\infty} dq' q'^2 \times \int_{-1}^{+1} dx' v(q, q', x, x') \frac{1}{E_{q_0} - E_{q'}} K(q', x', x_0). \tag{II.5}$$

Then the on-shell scattering amplitude can be gained through the one-dimensional integral equation in the angular space

$$T(q_0, x) = K(q_0, x, 1) - 2m\pi^2 q_0 i \int_{-1}^{+1} K(q_0, x, x')\, T(q_0, x'). \tag{II.6}$$

Instead of (II.5) a $K$-matrix $K(q, x)$ in analogy to Eq. (II.4) could have been introduced, which in the step (II.6), however, would have required interpolation.

As an example, typical for nuclear physics, we have chosen the local Malfliet–Tjon potential, MT III [3]

$$V(r) = (V_R e^{-\mu_R r} - V_A e^{-\mu_A r}) \frac{1}{r} \tag{II.7}$$

with $V_R = 1438.720$ MeV fm, $V_A = 626.885$ MeV fm, $\mu_R = 3.110\,\text{fm}^{-1}$, and $\mu_A = 1.550\,\text{fm}^{-1}$. In momentum space this yields

$$V(q, q', y) = \frac{1}{2\pi^2}\left(\frac{V_R}{q^2 + q'^2 - 2qq'y + \mu_R^2} - \frac{V_A}{q^2 + q'^2 - 2qq'y + \mu_A^2}\right) \tag{II.8a}$$

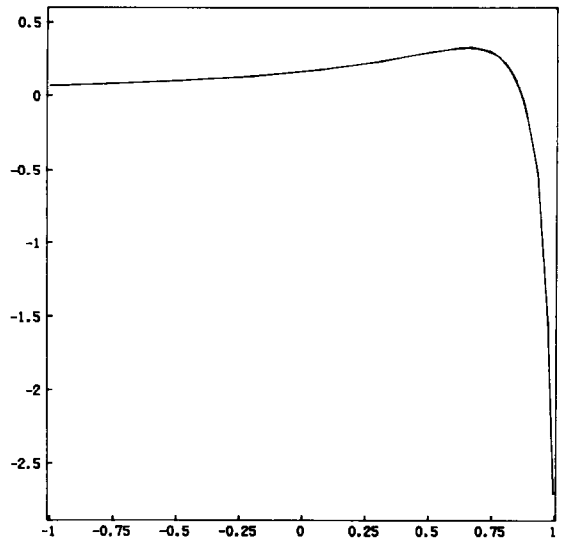


FIG 1 The real part of $T(q_0, x) * 10^2$ for $E_{q_0} = 697$ MeV against $x$

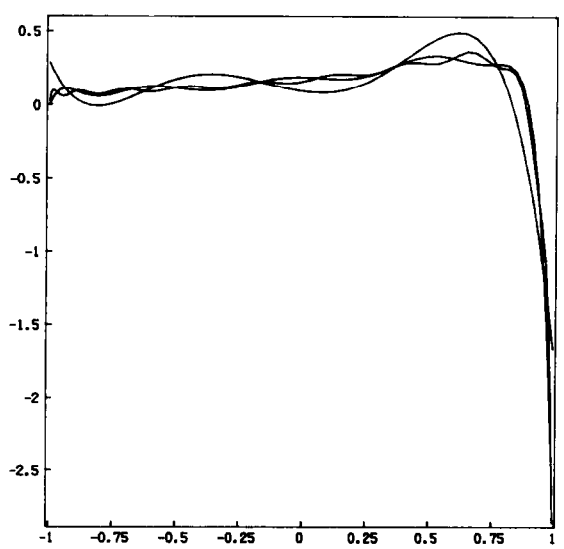


FIG 2 The real part of $T(q_0, x) * 10^2$ in a partial wave representation for $E_{q_0} = 697$ MeV against $x$ The three curves refer to $l_{max} = 5$, 10, and 20, respectively

or

$$v(q, q', x, x') = \frac{1}{\pi}\left(\frac{V_R}{\sqrt{(q^2+q'^2-2qq'xx'+\mu_R^2)^2-4q^2q'^2(1-x^2)(1-x'^2)}}\right.$$
$$\left.-\frac{V_A}{\sqrt{(q^2+q'^2-2qq'xx'+\mu_A^2)^2-4q^2q'^2(1-x^2)(1-x'^2)}}\right) \qquad \text{(II.8b)}$$

Equation (II.5) is easily solved using typically 20(14) quadrature points in $q(x)$. (We used the Padé technique to sum up the Neumann series.) The on-shell equation (II.6) then yields the scattering amplitude.

We show the real part of $T$ as a function of $x$ in Fig. 1. This is to be compared with Fig. 2, where the partial wave amplitudes summed up to $l_{\max} = 5$, 10, 20 are exhibited. They are defined by

$$T(q_0, x) = \frac{1}{2iq_0}\sum_{l=0}^{\infty} T_l(q_0)\, P_l(x). \qquad \text{(II.9)}$$

The complicated interference is obvious which has to build up the curve without wiggles of Fig. 1.

A generalization to particles with spin, for example the two-nucleon system, can easily be worked out. It leads to a finite small number of coupled equations in the variables $q$ and $x$. Its application to the two-nucleon system will be presented in a forthcoming paper.

## III. Time-Dependent Potential Scattering

The time-dependent Schrödinger equation can be cast into the form of an integral equation

$$\psi(t) = \psi_0(t) + \frac{1}{i}\int_{-\infty}^{t} dt' e^{-iH_0(t-t')}\, V\psi(t'). \qquad \text{(III.1)}$$

Here $\psi(t)$ coincides at $t = -\infty$ with the free wavepacket

$$|\psi_0(t)\rangle = \int d^3q\, |\mathbf{q}\rangle\, e^{-iE_q t} f_0(\mathbf{q}) \qquad \text{(III.2)}$$

We find the behaviour for $t \to +\infty$ by rewriting (III.1) into

$$\psi(t) = \psi_0(t) + \frac{1}{i}\int_{-\infty}^{+\infty} dt' e^{-iH_0(t-t')}\, V\psi(t')$$
$$-\frac{1}{i}\int_{t}^{\infty} dt' e^{-iH_0(t-t')}\, V\psi(t'). \qquad \text{(III.3)}$$

The second term on the right-hand side of (III.3) is evaluated with the help of the stationary scattering solutions $\psi_{\mathbf{q}}^{(+)}$ of the time-independent Schrödinger equation:

$$\psi(t) = \int d^3q \psi_{\mathbf{q}}^{(+)} e^{-iE_q t} f_0(\mathbf{q}). \tag{III.4}$$

One gets

$$\begin{aligned} &\frac{1}{i}\int_{-\infty}^{+\infty} dt' e^{-iH_0(t-t')} V\psi(t') \\ &\quad = \frac{1}{i}\int d^3q\, |\mathbf{q}\rangle\, e^{-iE_q t} \int d^3q' \langle \mathbf{q}\,|V|\,\psi_{\mathbf{q}'}^{(+)}\rangle \\ &\quad\quad \times \int_{-\infty}^{\infty} dt' e^{i(E_q - E_q)t'} f_0(\mathbf{q}') \qquad \text{(III.5)} \\ &\quad = \frac{1}{i}\int d^3q\, |\mathbf{q}\rangle\, e^{-iE_q t} \int d^3q' T(\mathbf{q}, \mathbf{q}') \\ &\quad\quad \times 2\pi\, \delta(E_q - E_{q'})\, f_0(\mathbf{q}'). \qquad \text{(III.6)} \end{aligned}$$

We encounter again the half-shell $T$-matrix

$$T(\mathbf{q}, \mathbf{q}') \equiv \langle \mathbf{q}\,|V|\,\psi_{\mathbf{q}'}^{(+)}\rangle \tag{III.7}$$

of Section II.

Let us regard the momentum space representation of (III.1) and (III.3). We define

$$\langle \mathbf{q}\,|\psi(t)\rangle \equiv f(\mathbf{q}, t) \tag{III.8}$$

$$\langle \mathbf{q}\,|\psi_0(t)\rangle \equiv f_0(\mathbf{q}, t) = e^{-iE_q t} f_0(\mathbf{q}) \tag{III.9}$$

and get

$$\begin{aligned} f(\mathbf{q}, t) &= e^{-iE_q t} f_0(\mathbf{q}) + \frac{1}{i}\int_{-\infty}^{t} dt' e^{-iE_q(t-t')} \\ &\quad \times \int d^3q' V(\mathbf{q}, \mathbf{q}')\, f(\mathbf{q}', t') \qquad \text{(III.10)} \\ f(\mathbf{q}, t) &= e^{-iE_q t} f_0(\mathbf{q}) - 2\pi i e^{-iE_q t} \\ &\quad \times \int d^3q' T(\mathbf{q}, \mathbf{q}')\, \delta(E_q - E_{q'})\, f_0(\mathbf{q}') \\ &\quad - \frac{1}{i}\int_{t}^{\infty} dt' e^{-iE_q(t-t')} \int d^3q' V(\mathbf{q}, \mathbf{q}')\, f(\mathbf{q}', t'). \qquad \text{(III.11)} \end{aligned}$$

Clearly, in a numerical treatment, the strong oscillations $e^{-\imath E_q t}$ connected with the flux and energy conserving asymptotic parts in (III.10) and (III.11) at large $|t|$ should be avoided. In (III.10) we could subtract the oscillating incoming part

$$f(\mathbf{q}, t) \equiv f_0(\mathbf{q}, t) + R_t(\mathbf{q}, t) \tag{III.12}$$

and consider the resulting integral equation for the scattered part $R_t(\mathbf{q}, t)$

$$R_t(\mathbf{q}, t) = \frac{1}{\imath}\int_{-\infty}^{t} dt' e^{-\imath E_q(t-t')} \int d^3q' V(\mathbf{q}, \mathbf{q}')\, e^{-\imath E_q t'} f_0(\mathbf{q}')$$

$$+\frac{1}{\imath}\int_{-\infty}^{t} dt' e^{-\imath E_q(t-t')} \int d^3q' V(\mathbf{q}, \mathbf{q}')\, R_t(\mathbf{q}', t') \tag{III.13}$$

Whereas for $t \to -\infty$, $R_t(\mathbf{q}, t)$ tends towards zero, for $t \to +\infty$ it oscillates according to the second term on the right-hand side of (III.11). An obvious remedy is to turn to the interaction representation and strip off the free time behaviour

$$\hat{R}_t(\mathbf{q}, t) \equiv e^{\imath E_q t} R_t(\mathbf{q}, t). \tag{III.14}$$

Then we arrive at

$$\hat{R}_t(\mathbf{q}, t) = \frac{1}{\imath}\int_{-\infty}^{t} dt' e^{\imath E_q t'} \int d^3q' V(\mathbf{q}, \mathbf{q}')\, e^{-\imath E_q t'} f_0(\mathbf{q}')$$

$$+\frac{1}{\imath}\int_{-\infty}^{t} dt' e^{\imath E_q t'} \int d^3q' V(\mathbf{q}, \mathbf{q}')\, e^{-\imath E_q t'} \hat{R}_t(\mathbf{q}', t') \tag{III.15}$$

Is $\hat{R}_t(\mathbf{q}, t)$ now free of oscillations at large $|t|$-values? We enlighten that question with the aid of the formal solution (III.4). In momentum representation we get

$$f(\mathbf{q}, t) = \int d^3q' \langle \mathbf{q} | \psi_{\mathbf{q}'}^{(+)} \rangle\, e^{-\imath E_q t} f_0(\mathbf{q}')$$

$$= e^{-\imath E_q t} f_0(\mathbf{q})$$

$$+ \int d^3q' \frac{T(\mathbf{q}, \mathbf{q}')}{E_{q'} + \imath\varepsilon - E_q} e^{-\imath E_q t} f_0(\mathbf{q}') \tag{III.16}$$

or

$$\hat{R}_t(\mathbf{q}, t) = \int d^3q' e^{\imath(E_q - E_{q'})t} \frac{T(\mathbf{q}, \mathbf{q}')}{E_{q'} + \imath\varepsilon - E_q} f_0(\mathbf{q}'). \tag{III.17}$$

Clearly for $|t| \to \infty$ the integral excluding the neighbourhood of the singularity vanishes due to the Riemann–Lebesgue lemma. The integral over a sufficiently small neighbourhood of $E_q$ can be easily evaluated by taking $T(\mathbf{q}, \mathbf{q}') f_0(\mathbf{q}')$ out of the integral. One finds that it vanishes for $t \to -\infty$ and approaches the expression

(III.6) for $t \to +\infty$, with the exponential factor $e^{-iE_q t}$ stripped off. This insight, however, is too weak, since we need to know *how* the asymptotic limits are approached. We regard a Gaussian momentum distribution in the initial state

$$f_0(\mathbf{q}) = \left(\frac{\sigma}{\sqrt{\pi}}\right)^{3/2} e^{-(\sigma^2/2)(\mathbf{q}-\mathbf{q}_0)^2}. \tag{III.18}$$

For $t>0$ ($t<0$) one turns the path of integration in (III.17) into the angular directions $-\pi/4$ ($+\pi/4$) (see Fig. 3). Thereby for $t>0$ one picks up a residue at $|\mathbf{q}'| = |\mathbf{q}| - i\varepsilon$ which provides the leading asymptotic part:

$$\begin{aligned}\hat{R}_t(\mathbf{q}, t) = &-2\pi i\theta(t) \int d^3q' T(\mathbf{q}, \mathbf{q}')\, \delta(E_q - E_{q'}) f_0(\mathbf{q}') \\ &+ e^{iE_q t}(1 \pm i) \int d^3l' e^{-l'^2(|t|/m)} \frac{T(\mathbf{q}, \mathbf{l}'(1 \pm i))}{i(l'^2/m) + i\varepsilon - E_q} \\ &\times \left(\frac{\sigma}{\sqrt{\pi}}\right)^{3/2} e^{-\sigma^2/2(2il'^2 - 2\mathbf{q}_0 \cdot \mathbf{l}' \mp 2i\mathbf{q}_0 \cdot \mathbf{l}' + q_0^2)},\end{aligned} \tag{III.19}$$

where we put $\mathbf{q}' = \mathbf{l}(1 \pm i)$ for $t \lessgtr 0$.

To keep our analysis as simple as possible we have assumed that the $t$-matrix has no poles or cuts in the dashed regions of Fig. 3. In the more general case when there are poles in the respective region one has to add some residues. These additional terms, however, decrease exponentially with $|t|$.

In the second term in (III.19) we take an averaged value of the $t$-matrix and the propagator, $c(\mathbf{q})$, out of the integral and end up with

$$\begin{aligned}\hat{R}_t(\mathbf{q}, t) = &-2\pi i\theta(t) \int d^3q' T(\mathbf{q}, \mathbf{q}')\, \delta(E_q - E_{q'}) f_0(\mathbf{q}') \\ &+ e^{iE_q t} c(\mathbf{q})\, \Phi(t)\end{aligned} \tag{III.20}$$

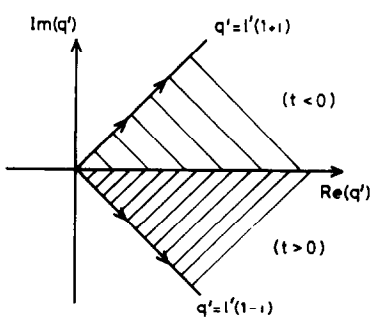


FIG 3 Contour deformations for (III 17) as explained in the text

with

$$\Phi(t) = \int d^3q' e^{-iE_{q'}t} f_0(\mathbf{q}')$$

$$= \left[\frac{2\pi}{\sigma\sqrt{\pi}\,(1 + i(t/m\sigma^2))}\right]^{3/2} e^{-iE_{q_0}t} \exp\left\{\frac{-(q_0^2/2\sigma^2m^2)t^2}{1 + i(t/m\sigma^2)}\right\}. \qquad \text{(III.21)}$$

$\Phi(t)$ is just the free wave packet in configuration space at the place $\mathbf{x} = 0$ with a spreading

$$\xi = \frac{t}{m\sigma^2}. \qquad \text{(III.22)}$$

It can be seen from (III.19) that $c(\mathbf{q})$ will depend only weakly on $t$. Neglecting that dependence we see that for $|\xi| \ll 1$, $\hat{R}_t(\mathbf{q}, t)$ approaches its asymptotic value in $t$ rather quickly: $\Phi(t) \sim e^{-(q_0^2/2\sigma^2m^2)t^2}$. Let us take the example to be discussed in chapter IV:

$$q_0 = 3.5\ \text{fm}^{-1}, \qquad \sigma = 5\ \text{fm}, \qquad m = 2.379\ \text{fm}^{-1}.$$

$\sigma$ is the width of the initial wavepacket in configuration space. Assuming a potential range of $\approx 3$ fm (see (II.7)) we therefore have no considerable overlap of the wavepacket and the interaction region at time $|t| \approx 20$ fm. This corresponds to $|\xi| = 0.34$ and thus $\Phi(t)$ decreases like a Gaussian in $|t|$. The numerical investigations in Section IV confirm these results completely. It is not necessary to go to the far asymptotic region with $|\xi| \gg 1$, where the second term in (III.20) shows the well-known decrease proportional to $|t|^{-3/2}$. In the example above we see that the exponential factors in (III.21) tend towards $e^{-(1/2)q_0^2\sigma^2} \approx 10^{-67}$ for large $|t|$.

Summarizing we can say that the use of an initial wavepacket in *Gaussian form* gives rise to the very strong decreases of the function $\hat{R}_t$ to its asymptotic value.

Thus a numerical calculation of $\hat{R}_t$ by an appropriately modified integral equation (III.13) appears possible. In reality the factor $e^{iE_{q'}t}$ in (III.20) causes strong oscillations even in the case of intermediate times ($t \approx 10$ fm in the example above). Moreover, the appropriate integral equation for $\hat{R}_t$ is much more difficult to solve than the one for the Schrödinger amplitude $R_t$ (see Section IV). If we go back to $R_t$ we can push this oscillating factor to the flux conserving asymptotic part, which is subtracted out anyhow for $t < 0$. For $t > 0$, however, this part is not known and cannot be subtracted out. We investigated two ways to solve that difficulty, which we now present in turn.

(a) *Forward and Backward Propagation in Time*

Starting at large negative times with the initial wavepacket we follow the evolution of the wavefunction till $t = 0$. Then we start at large positive times with a suitable set of wavepackets directed towards the potential area and coming from all

directions, and follow their evolution till $t=0$. The latter set of states has to be complete enough to build $\psi(0)$ by a linear combination. Equating that linear combination to $\psi(0)$ gained through negative times determines the on-shell scattering amplitude.

For $t<0$ we use (III.13). According to the consideration above we know that $R_t(\mathbf{q}, t)$ approaches zero for $t \to -\infty$ without strong oscillations. For $t>0$ we use (III.11). Contrary to the case $t<0$ we do not know the driving term. But we can parametrise it with the aid of a suitable set of known functions $H_\alpha(\mathbf{q})$:

$$f_0(\mathbf{q}) - 2\pi i \int d^3q' T(\mathbf{q}, \mathbf{q}')\, \delta(E_q - E_{q'})\, f_0(\mathbf{q}')$$

$$\equiv \sum_\alpha H_\alpha(\mathbf{q})\, c_\alpha. \tag{III.23}$$

Then defining

$$f(\mathbf{q}, t) = e^{-iE_q t} \sum_\alpha H_\alpha(\mathbf{q})\, c_\alpha + R_f(\mathbf{q}, t)$$

we get

$$\begin{aligned} R_f(\mathbf{q}, t) = & -\frac{1}{i} \int_t^\infty dt' e^{-iE_q(t-t')} \\ & \times \int d^3q' V(\mathbf{q}, \mathbf{q}')\, e^{-iE_q t'} \sum_\alpha H_\alpha(\mathbf{q}')\, c_\alpha \\ & -\frac{1}{i} \int_t^\infty dt' e^{-iE_q(t-t')} \int d^3q' V(\mathbf{q}, \mathbf{q}')\, R_f(\mathbf{q}', t'). \end{aligned} \tag{III.24}$$

Clearly $R_f(\mathbf{q}, t)$ can be written as

$$R_f(\mathbf{q}, t) = \sum_\alpha R_\alpha(\mathbf{q}, t)\, c_\alpha, \tag{III.25}$$

where $R_\beta(\mathbf{q}, t)$ obeys (III.24) with $c_\alpha = \delta_{\alpha\beta}$. Again we know that $R_f(\mathbf{q}, t)$ approaches zero at $t \to +\infty$ without strong oscillations. We determine the coefficients $c_\alpha$ knowledge acquired at $t=0$ from both sides:

$$\sum_\alpha H_\alpha(\mathbf{q})\, c_\alpha + R_f(\mathbf{q}, 0) = f_0(\mathbf{q}) + R_t(\mathbf{q}, 0). \tag{III.26}$$

Choosing appropriate $\mathbf{q}$-values yields a sufficient number of equations to determine the coefficients $c_\alpha$ and therefore the on-shell $T$-matrix according to (III.23).

We tested that procedure in one space dimension using a Gauss potential

$V(q, q') = -\lambda \exp\{-\beta^2(q-q')^2\}$ and an initial wavepacket $f_\circ(q)$ in Gaussian form as in (III.18). As the test functions $H_\alpha$ we choose

$$H_\alpha(q) = \begin{cases} q^{\alpha-1} f_0(q) & (\alpha \geqslant 1) \\ f_0(q) & (\alpha = 0) \\ (-q)^{-\alpha-1} f_0(-q) & (\alpha \leqslant -1) \end{cases} \tag{III.27}$$

(We put $c_0 = 1$ in the trivial case $\alpha = 0$.)

We calculated $R_t(q, 0)$ according to (III.13) and $R_\alpha(q, 0)$ according to (III.24) and (III.25). The time integration was handled by cubic spline interpolation as described in the Appendix. With the help of the coefficients $c_\alpha$ (obtained from (III.26)) one easily calculated the on-shell $T$-matrix for several momenta $q$ contained in the initial wavepacket (see III.23). In order to achieve an accuracy of two digits in the on-shell $t$-matrix elements it proved sufficient to use $|\alpha| \leqslant 3$ in (III.27).

Since (III.24) has to be solved for each value of $\alpha$, a parallel vector processing would be ideal This would be even more relevant in the three-dimensional case, where one has to approximate $f(\mathbf{q}, t \to \infty)$ by many more functions $H_\alpha(\mathbf{q})$ in three dimensions. A successful use of that method depends therefore on whether one can find an optimal set of test functions $H_\alpha(\mathbf{q})$. Instead of diving into that problem we studied another method relying on the time-integration from $t = -\infty$ to $t = +\infty$ as described in the next section.

(b) *Contour Deformation*

The asymptotic estimate (III.20) of the formal solution (III.17) suggests another possibility to get rid of the oscillations. We go back to the Schrödinger amplitude $R_t(\mathbf{q}, t) = e^{-iE_q t} \hat{R}_t(\mathbf{q}, t)$ and use complex momenta $\mathbf{q} \to \mathbf{l}(1-i)$. Then $R_t(\mathbf{q}, t) \to e^{-l^2(t\,m)} \hat{R}_t(\mathbf{l}(1-i), t)$ is well defined and *not* oscillating, provided that the $T$-matrix allows such a change to complex momenta. (Note that the $\theta$-function in the first term of (III.20) prevents the appearance of an exponentially increasing factor $e^{-l^2(t\,m)}$ in the case of negative $t$-values).

Unfortunately, when shifting the momenta into the complex plane as described above one may hit singularities of the potential. This is the case in nuclear physics where boson exchanges characterize the analytical structure of $V(\mathbf{q}, \mathbf{q}')$. A typical term is

$$V(\mathbf{q}, \mathbf{q}') \sim \frac{1}{\mu^2 + (\mathbf{q}-\mathbf{q}')^2} = \frac{1}{\mu^2 + q^2 - 2qq' \cos\theta + q'^2} \tag{III.28}$$

which in the worst case ($\cos\theta = 1$) has a pole at $q = q' \pm i\mu$. Therefore as a first step we choose both $\mathbf{q}$ and $\mathbf{q}'$ in (III.13) of the form $\mathbf{l}(1 - i\alpha)$ with $0 \leqslant \alpha \leqslant 1$ and get

$$R_t(\mathbf{l}(1-i\alpha), t) = R_0(\mathbf{l}(1-i\alpha), t) + \frac{1}{i}\int_{-\infty}^{t} dt' e^{-il^2(1-\alpha^2)((t-t')/2m)}\, e^{-\alpha l^2((t-t')/m)} \times (1-i\alpha)\int d^3l' V(\mathbf{l}(1-i\alpha), \mathbf{l}'(1-i\alpha)) \times R_t(\mathbf{l}'(1-i\alpha), t'). \tag{III.29}$$

The kernel in (III.29) is well behaved for all $\alpha$'s and guarantees the existence of $R_t(\mathbf{l}(1-i\alpha), t)$, provided the driving term $R_0$ exists.

Once $R_t(\mathbf{l}(1-i\alpha), t)$ is determined we use (III.13) again to find the Schrödinger amplitude for real momenta

$$R_t(\mathbf{q}, t) = R_0(\mathbf{q}, t) + \frac{1}{i}\int_{-\infty}^{t} dt' e^{-iE_q(t-t')}(1-i\alpha) \times \int d^3l' V(\mathbf{q}, \mathbf{l}(1-i\alpha))\, R_t(\mathbf{l}'(1-i\alpha), t'). \tag{III.30}$$

This equation is only correct for $0 \leqslant \alpha \leqslant \mu/q$ as is obvious from (III.28). Otherwise a residue at the pole of the potential would have to be taken into account. Though this is possible it would be against the spirit of our approach: We do not want to replace propagator singularities (occurring in a time-independent approach) by potential singularities. If the maximum value of $q$ (real) is greater than $\mu$ we therefore content ourselves with $\alpha$ less than 1 (see (III.33) below.)

Returning now to (III.29) we recognize that in the case $\alpha < 1$ the kernel still shows an oscillating behaviour but it is strongly damped by the factor $e^{-\alpha l^2((t-t')/m)}$ in the case of large $l$-values. That factor also suppresses the contributions of $R_t(\mathbf{l}'(1-i\alpha), t')$ for $t' \ll t$. Thus numerical errors in $R_t$ do not pile up.

The driving term $R_0$ reads

$$R_0(\mathbf{l}(1-i\alpha), t) = \frac{1}{i}\int_{-\infty}^{t} dt' e^{-il^2(1-\alpha^2)((t-t')/2m)}\, e^{-\alpha l^2((t-t')/m)} \times \int_{q_0-\Delta}^{q_0+\Delta} dq' q'^2 V(\mathbf{l}(1-i\alpha), q'\hat{q}_0)\, e^{-iE_{q'}t} f_0(q'). \tag{III.31}$$

Here we used an initial wavepacket in the form

$$f_0(\mathbf{q}) = \delta^2(\hat{q}-\hat{q}_0) f_0(q)$$

$$f_0(q) = \begin{cases} \left(\frac{\sigma}{\sqrt{\pi}}\right)^{3/2} \exp\left\{-\frac{\sigma^2}{2}(q-q_0)^2\right\} & \text{if } q_0-\Delta \leqslant q \leqslant q_0+\Delta \\ 0 & \text{else.} \end{cases} \tag{III.32}$$

The delta functional in the direction of $\hat{q}_0$ was introduced in order to make the calculation as simple as possible. The differences between this wavepacket and the pure Gaussian one in (III.18) only lead to small modifications of the analytical discussion in (III.19)–(III.21).

As above we have supposed that $\alpha < \mu/q'$ for all $q'$ in order to avoid a singularity from the potential. Thus $\alpha$ is restricted by the maximal $q$-value in the initial wavepacket

$$0 < \alpha < \frac{\mu}{q_0 + \Delta}. \tag{III.33}$$

We use (III.30) to determine the amplitud for real $q$-values. Physically interesting and present at large positive times $t$ are only momenta from the initial momentum distribution. For those $q$-values the choice (III.33) also guarantees the existence of (III.30).

The complex path of integration $C$ ($q' = l'(1 - i\alpha)$) in (III.29) and (III.30) is shown in Fig. 4. These equations can be simplified. It is clear that $R_l(\mathbf{q}, t)$ only depends on $\mathbf{q}^2$ and $x = \hat{q} \cdot \hat{q}_0$. Therefore the azimuthal angle $\varphi$ occurs only in the potential and we can proceed as in Section II by defining $v$ (see (II.3)). We then get

$$R_l(q, x, t) = R_0(q, x, t) + \frac{1}{i} \int_{-\infty}^{t} dt' e^{-iE_q(t - t')} \times \int_C dq' q'^2 \int_{-1}^{+1} dx' v(q, q', x, x') R_l(q', x', t'). \tag{III.34}$$

If $q$ is real this represents (III.30). For $q$ along $C$ this is the integral equation (III.29) to be solved, which will be described in the next section.

To demonstrate the advantage of complex $q$-values we compare the Schrödinger amplitudes $R_l(q, x, t)$ for complex and real momenta in Figs. 5 and 6. For a fixed angle $x$ the time development of the real part of $R_l$ is shown. The underlying

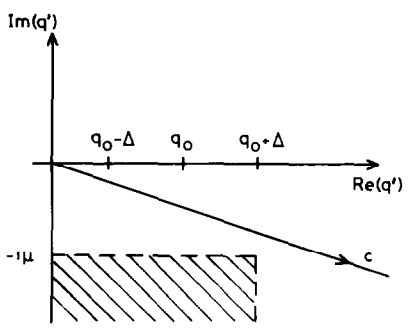


FIG 4. The complex path of integration $C$ in equations (III 29), (III 30), (III 34) The range of initial momenta is indicated together with the region where potential singularities occur.

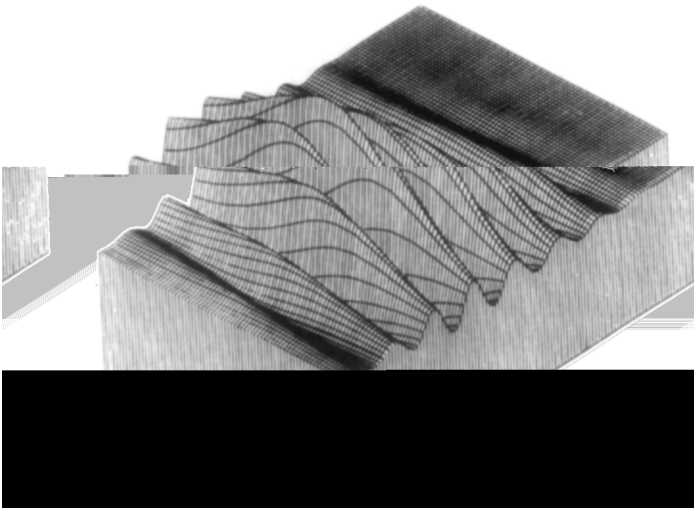

FIG 5 The real part of $R_\lambda(q, x, t)$ for complex momenta and fixed $x$ between $t = -10$ fm and $t = 15$ fm The $x$- and $y$-axis denote time and momentum, respectively

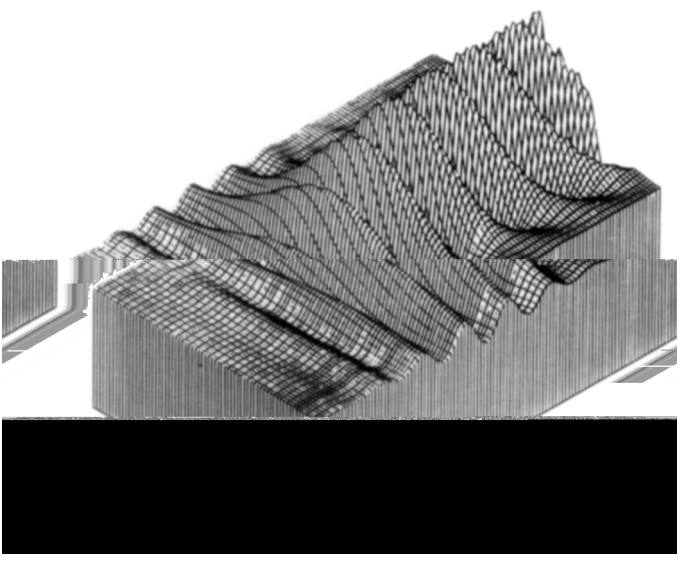

FIG 6 The same as in Fig 5 for real momenta

physical example will be explained in Section IV. Whereas $R_t$ along $C$ gets smaller for large $t$-values it oscillates strongly for real $q$-values. These strong oscillations make a direct solution of (III.13) for real $q$-values very difficult if not impossible.

Having obtained $R_t(q, x, t)$ for real $q$ and $t \to \infty$ we can extract the $T$-matrix $T(\mathbf{q}, \mathbf{q}')$ using (III.11) and (III.12):

$$\hat{R}_t(\mathbf{q}, t) = e^{tE_q t} R_t(\mathbf{q}, t)$$

$$\xrightarrow[t \to \infty]{} -2\pi i \int d^3q' T(\mathbf{q}, \mathbf{q}')\, \delta(E_q - E_{q'})\, f_0(\mathbf{q}'). \tag{III.35}$$

Inserting our special wavepacket (III.32) we finally get

$$\hat{R}_t(\mathbf{q}, t \to \infty) = -2\pi i m q T(\mathbf{q}, q \cdot \hat{q}_0)\, f_0(q)$$

$$\equiv -2\pi i m q T(q, \hat{q} \cdot \hat{q}_0)\, f_0(q). \tag{III.36}$$

## IV. Numerical Treatment of the Time Dependent Schrodinger Equation

The integral equation (III.34) poses a problem in three variables: $q$, $x$, $t$. Since for general interactions we cannot expect that it can be solved by iteration (Born series), we have to invert a matrix whose rows and columns are numbered by the set of $q$-, $x$-, and $t$-values. In order to avoid too large matrices we split the total time interval into $N$ parts, $\Delta T = 2T_0/N$, where $\mp T_0$ are the times beyond that the in- and outgoing wavepackets can be assumed to be free. Equation (III.34) is then solved in steps for the consecutive time intervals $\Delta T$.

Let $T$ be the left end of such an interval $\Delta T$. Then Eq. (III.34) can obviously be rewritten into

$$R_t(q, x, t) = R_0^{(T)}(q, x, t) + \frac{1}{t} \int_T^t dt' e^{-iE_q(t - t')}$$

$$\times \int_C dq' q'^2 \int_{-1}^{+1} dx' v(q, q', x, x')\, R_t(q', x', t') \tag{IV.1}$$

with (see (III.31))

$$R_0^{(T)}(q, x, t) = e^{-iE_q(t - T)}\, R_t(q, x, T) + \int_{q_0 - \Delta}^{q_0 + \Delta} dq' q'^2 e^{-iE_q t}$$

$$\times \frac{e^{-i(E_q - E_q)(t - T)} - 1}{E_q - E_q} \frac{1}{2\pi} v(q, q', x, 1)\, f_0(q' - q_0). \tag{IV.2}$$

Equation (IV.1) is used for $T \leqslant t \leqslant T + \Delta T$. The resulting function $R_t(q, x, T + \Delta T)$ is the starting function for the following interval. At $T = -T_0$ (i.e., in the first interval) we can put $R_t(q, x, -T_0) \equiv 0$.

Equation (IV.1) has now to be discretized in the three variables $q$, $x$, and $t$. We start the discussion with the $t$-dependence. If $\Delta T$ is sufficiently small one can think of a linear interpolation in $t$ for $t \in [T, T+\Delta T]$,

$$R_i(q, x, t) = R_i(q, x, T)\, N_{21}(t) + R_i(q, x, T+\Delta T)\, N_{22}(t) \tag{IV.3}$$

with

$$\begin{aligned} N_{21}(t) &= \frac{T+\Delta T - t}{\Delta T} \\ N_{22}(t) &= \frac{t-T}{\Delta T}. \end{aligned} \tag{IV.4}$$

$R_i(q, x, T+\Delta T)$ is now simply calculated by putting $t = T+\Delta T$ in (IV.1) and inserting (IV.3) into the $t'$-integral on the right side. The $t'$-integral then reduces to two trivial integrals:

$$\begin{aligned} K_{2i}(z, \Delta T) &= \int_T^{T+\Delta T} dt' e^{-z(T+\Delta T - t')} N_{2i}(t') \\ &= \frac{1}{z} \begin{cases} \dfrac{1}{z\,\Delta T} - \left(1 + \dfrac{1}{z\,\Delta T}\right) e^{-z\Delta T} & (i=1) \\ \left(1 - \dfrac{1}{z\,\Delta T}\right) + \dfrac{1}{z\,\Delta T} e^{-z\Delta T} & (i=2). \end{cases} \end{aligned} \tag{IV.5}$$

This leads to the integral equation

$$\begin{aligned} R_i(q, x, T+\Delta T) = R_0^{(T)}(q, x, T+\Delta T) &+ \frac{1}{i} K_{21}(iE_q, \Delta T) \int_C dq' q'^2 \\ &\times \int_{-1}^{+1} dx' v(q, q', x, x')\, R_i(q', x', T) + \frac{1}{i} K_{22}(iE_q, \Delta T) \\ &\times \int_C dq' q'^2 \int_{-1}^{+1} dx' v(q, q', x, x')\, R_i(q', x', T+\Delta T). \end{aligned} \tag{IV.6}$$

Suppose now that the double integral in $q'$ and $x'$ has been discretized (we use Gaussian quadrature points for that purpose),

$$\int_C dq' q'^2 \int_{-1}^{+1} dx' v(q, q', x, x')\, R_i(q', x', t) \approx \sum_\beta V_{\alpha\beta} R_{i\beta}(t), \tag{IV.7}$$

where the indices $\alpha$ and $\beta$ number all discrete values of the set $(q, x)$ and $(q', x')$, respectively. Then equation (IV.6) reduces to a system of linear equations

$$\sum_\beta M_{\alpha\beta}^{(2)} R_{i\beta}(T+\Delta T) = R_{0\alpha}^{(T)}(T+\Delta T) + \sum_\beta M_{\alpha\beta}^{(1)} R_{i\beta}(T) \tag{IV.8}$$

with two matrices

$$M^{(1)}_{\alpha\beta} = \frac{1}{i} K_{21}(iE_{q_z}, \Delta T) V_{\alpha\beta}$$
$$M^{(2)}_{\alpha\beta} = \delta_{\alpha\beta} - \frac{1}{i} K_{22}(iE_{q_z}, \Delta T) V_{\alpha\beta}. \tag{IV.9}$$

Note that neither $M^{(1)}_{\alpha\beta}$ nor $M^{(2)}_{\alpha\beta}$ depends on the time interval chosen, i.e., on the value of $T$!

So we have to calculate $M^{(1)}_{\alpha\beta}$ and $M^{(2)}_{\alpha\beta}$ and invert $M^{(2)}_{\alpha\beta}$ only *once* for *all* intervals $[T, T+\Delta T]$: Once we have made a LU-decomposition of $M^{(2)}_{\alpha\beta}$ we just apply the decomposed matrix to the right-hand side of (IV.8).

Linear interpolation in the case of badly behaved functions $R_l(q, x, t)$ requires a small $\Delta T$, and a lot of steps are necessary to go from $-T_0$ to $+T_0$. In such a case it may be better to use a more accurate interpolation.

In the following, we present an interpolation by cubic polynomials. The treatment is strongly influenced by cubic B-splines, which provide us with a still better way of interpolating the $t$-dependence and which are treated in the Appendix.

Choose the following set of linearly independent cubic polynomials in the interval $[T, T+\Delta T]$:

$$N_{41}(t) = \left(\frac{T+\Delta T-t}{\Delta T}\right)^3$$
$$N_{42}(t) = 3\left(\frac{T+\Delta T-t}{\Delta T}\right)^2\left(\frac{t-T}{\Delta T}\right)$$
$$N_{43}(t) = 3\left(\frac{T+\Delta T-t}{\Delta T}\right)\left(\frac{t-T}{\Delta T}\right)^2 \tag{IV.10}$$
$$N_{44}(t) = \left(\frac{t-T}{\Delta T}\right)^3$$

These polynomials can be generated by a simple recipe:

$$1 \equiv \left[\frac{(T+\Delta T-t)+(t-T)}{\Delta T}\right]^3 \equiv \sum_{l=1}^{4} N_{4l}(t). \tag{IV.11}$$

In a similar manner we can generate three quadratic polynomials

$$1 \equiv \left[\frac{(T+\Delta T-t)+(t-T)}{\Delta T}\right]^2 \equiv \sum_{l=1}^{3} N_{3l}(t) \tag{IV.12}$$

and the two linear polynomials $N_{2l}$ (see (IV.4)). These equations can be summarized into

$$N_{ni}(t) = \binom{n-1}{i-1}\left(\frac{T+\Delta T-t}{\Delta T}\right)^{n-i}\left(\frac{t-T}{\Delta T}\right)^{i-1}. \tag{IV.13}$$

From this one easily verifies

$$\dot{N}_{ni}(t) = \frac{n-1}{\Delta T}\left(N_{n-1,i-1}(t) - N_{n-1,i}(t)\right). \tag{IV.14}$$

With the ansatz

$$R_i(q, x, t) = \sum_{k=1}^{4} c_k(q, x)\, N_{4k}(t) \tag{IV.15}$$

the $t'$-integral in (IV.1) can be carried through analytically. In analogy to (IV.5) we define

$$K_{nk}(z, T, t) := \int_T^t dt' e^{-z(t-t')} N_{nk}(t'). \tag{IV.16}$$

Partial integration then leads to

$$K_{nk}(z, T, t) = \frac{1}{z}\left\{N_{nk}(t) - e^{-z(t-T)} N_{nk}(T) - \int_T^t dt' e^{-z(t-t')} \dot{N}_{nk}(t')\right\}. \tag{IV.17}$$

With the help of (IV.14) one obtains the recurrence relations

$$K_{nk}(z, T, t) = \frac{1}{z}\left\{N_{nk}(t) - e^{-z(t-T)} N_{nk}(T) - \frac{n-1}{\Delta T} K_{(n-1),(k-1)}(z, T, t) + \frac{n-1}{\Delta T} K_{(n-1),k}(z, T, t)\right\} \tag{IV.18}$$

which starts with the trivial case ($N_{11} \equiv 1$):

$$K_{11}(z, T, t) = \int_T^t dt' e^{-z(t-t')} = \frac{1}{z}(1 - e^{-z(t-T)}). \tag{IV.19}$$

Again, the integrals are independent from the time interval chosen. Indeed,

$$\tilde{K}_{nk}(z, T+\Delta T, t+\Delta T) = \int_{T+\Delta T}^{t+\Delta T} dt' e^{-z(t+\Delta T-t')} \tilde{N}_{nk}(t') = \int_T^t dt'' e^{-z(t-t'')} \tilde{N}_{nk}(t''+\Delta T), \tag{IV.20}$$

where the tilde indicates that both $\tilde{K}_{nk}$ and $\tilde{N}_{nk}$ refer to the shifted interval $[T+\Delta T, T+2\Delta T]$. As is obvious from (IV.13)

$$\tilde{N}_{nk}(t+\Delta T) = N_{nk}(t) \tag{IV.21}$$

and consequently

$$\tilde{K}_{nk}(z, T+\Delta T, t+\Delta T) = K_{nk}(z, T, t). \tag{IV.22}$$

We are now prepared to approximate the integral equation (IV.1) in the interval $[T, T+\Delta T]$:

$$\sum_{k=1}^{4} c_k(q, x)\, N_{4k}(t) = R_0^{(T)}(q, x, t) + \frac{1}{i} \sum_{k=1}^{4} K_{4k}(iE_q, T, t) \times \int_C dq' q'^2 \int_{-1}^{+1} dx' v(q, q', x, x')\, c_k(q', x'). \tag{IV.23}$$

In order to determine the four coefficients $c_k(q, x)$ $(k = 1, ..., 4)$ we need four $t$-values within the interval under consideration; we choose

$$t_j = T + (j-1)\frac{\Delta T}{3} \qquad (j = 1, .., 4). \tag{IV.24}$$

Finally, having discretized the integrals in $q'$ and $x'$ as in (IV.7) we end up with the following algebraic system of linear equations

$$\sum_{k=1}^{4} c_{k\alpha} N_{4k}(t_j) - \frac{1}{i} \sum_{k=1}^{4} K_{4k}(iE_{q_\alpha}, T, t_j) \sum_{\beta} V_{\alpha\beta} c_{k\beta} = R_{0\alpha}^{(T)}(t_j) \tag{IV.25}$$

Because of (IV.22), the construction and the LU-decomposition of the integral kernel have to be performed only once for *all* time invervals.

Note, however, that now the rank $n$ of the kernel is four times larger than in the case of linear interpolation because $R_i$ is calculated at four times $t_j$ simultaneously. The time required for the LU-decomposition is approximately proportional to $n^3$. This larger consumption of time has to be weighted against the smaller number of iterations (compared with linear interpolation). The choice for one of both methods naturally depends on the smoothness of the function $R_t$ and the size of the whole interval $[-T_0, T_0]$ (i.e., the necessary number of time steps) and on the value of $n$. Examples will be given below.

Let us now present an application. We choose again the Malfliet–Tjon potential considered in Section II. The initial momentum distribution is taken in the form (III.32). With $q_0 = 3.5\,\mathrm{fm}^{-1}$ which corresponds to a central energy $E_0 = 508$ MeV (we use a reduced mass for two nucleons of $m = 2.379\,\mathrm{fm}^{-1}$), $\Delta = 1.2\,\mathrm{fm}^{-1}$, and the

spread in configuration space is chosen to be ... 5 fm. Therefore all momenta between $q_{min}$ and $q_{max}$ occur in our wavepacket. (These high energies require, of course, a relativistic framework. Since we work in momentum space that change could be incorporated. Our aim, however, is to demonstrate the time-dependent and three-dimensional treatment without partial wave decomposition and we do not want to introduce unnecessary complications.)

A starting time of $T_0 = -20$ fm proved to be sufficient in order to get a stable result for the $T$-matrix extracted at $t = +20$ fm. We solved (IV. 1) for consecutive time intervals $\Delta T = 0.05$ fm by linear interpolation (see Eqs. (IV.3)–(IV.9)). Along the path $C$ of Fig. 4 ($\alpha = 0.3$) we used 39 Gaussian quadrature points in $q$ and 13 quadrature points in $x$. In this case the solution of (IV.1) takes about 230 s on a Cyber 205. The remaining steps to arrive at the $T$-matrix for energies contained in the initial wavepacket are negligible. The time development of $R_l(q, x, t)$ for complex $q$-values in comparison to real ones is shown in Figs. 5 and 6. In Table I we present the $T$-matrix for three energies contained in our wavepacket and several angles in comparison with results obtained with the time-independent calculation of Section II.

It is interesting to regard also how the angular distribution in $R_l(q, x, t)$ builds up in time. This is shown in Figs. 7 and 8 for a fixed real and complex momentum value $q$, respectively. Whereas for a real $q$-value the amplitude remains oscillating for large times it is damped for a complex momentum value.

In Table II we present the same example as above calculated in three different interpolation schemes: linear interpolation, interpolation by cubic polynomials, and interpolation by cubic splines with 7 knots (i.e., $m = 7$ in the appendix). The time intervals $\Delta T$ are chosen in such a way that all methods give nearly the same

TABLE I

The On-Shell $T$-Matrix $T(q, x) = |T(q, x)| \exp[i\varphi(q, x)]$ as Obtained from Time-Dependent (I) and Time-Independent (II) Calculations

| | | | I | | II | |
|---|---|---|---|---|---|---|
| $\frac{E_q}{\text{MeV}}$ | $\frac{q}{\text{fm}^{-1}}$ | $x$ | $\lvert T(q, x)\rvert$ | $\varphi(q, x)$ | $\lvert T(q, x)\rvert$ | $\varphi(q, x)$ |
| 300 | 2.69 | −1 | $1.43 * 10^{-3}$ | 0 01 | $1 43 * 10^{-3}$ | 0 01 |
| | | 0 | $2 77 * 10^{-3}$ | 0 41 | $2 76 * 10^{-3}$ | 0 41 |
| | | +1 | $32 1 * 10^{-3}$ | −2 91 | $32 0 * 10^{-3}$ | −2 91 |
| 500 | 3 47 | −1 | $1 21 * 10^{-3}$ | −0 52 | $1.22 * 10^{-3}$ | −0.52 |
| | | 0 | $2 08 * 10^{-3}$ | 0 07 | $2 08 * 10^{-3}$ | 0 07 |
| | | +1 | $31 8 * 10^{-3}$ | −2 95 | $31 8 * 10^{-3}$ | −2.95 |
| 700 | 4 11 | −1 | $1 04 * 10^{-3}$ | −0 83 | $1 05 * 10^{-3}$ | −0 82 |
| | | 0 | $1.73 * 10^{-3}$ | −0 23 | $1 73 * 10^{-3}$ | −0.23 |
| | | +1 | $31 5 * 10^{-3}$ | −2 97 | $31 6 * 10^{-3}$ | −2 97 |

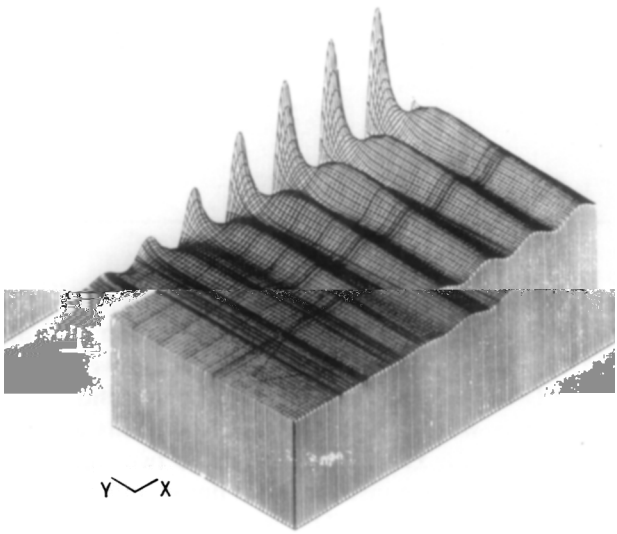


FIG 7 The real part of $R_t(q, x, t)$ against $x = \hat{q}\ \hat{q}_0$ for a fixed real momentum between $t = -10$ fm and $t = 10$ fm The $x$- and $y$-axis denote time and $\hat{q}\ \hat{q}_0$, respectively

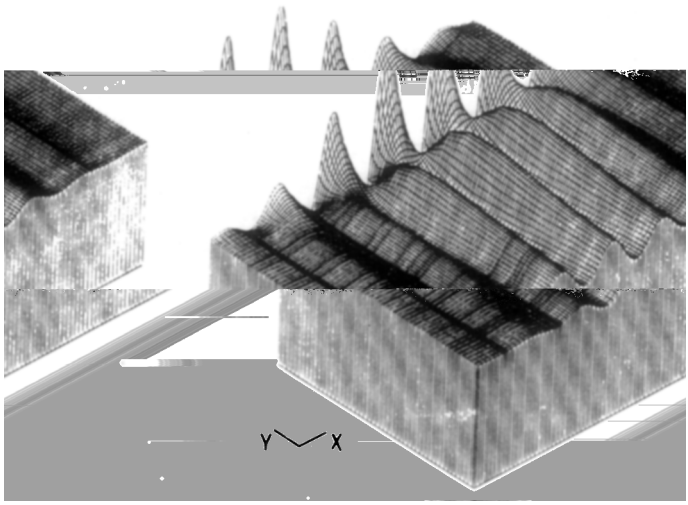


FIG 8 The same as in Fig 7 for a fixed complex momentum

TABLE II

Comparison of Three Different Time-Interpolation Schemes

| | Linear interpolation | Interpolation by cubic polynomials | Interpolation by cubic splines (7 knots) |
|---|---|---|---|
| $\Delta T$/fm | 0 125 | 0.75 | 3 |
| $\Delta t'$/fm | 0 125 | 0 25 | 0 5 |
| $T_{\text{lu}}$/s | 1 | 59 | 292 |
| $T_{\text{total}}$/s | 70 | 120 | 320 |

accuracy in the final result (at least in the neighbourhood of $q_0$). Note the great differences in the distances $\Delta t'$ between adjacent interpolation points! ($\Delta t' = t_j - t_{j-1}$ in (IV.23) or (A.16); in the case of linear interpolation we naturally have $\Delta t' = \Delta T$.) We give the CPU times used for the LU-decomposition and for the whole calculation. For simplicity we just worked with 28 $q'$-points and 9$x'$-points; in this case the results for the $T$-matrix were accurate up to two significant digits.

The numbers $T_{\text{total}}$ in Table II demonstrate that linear interpolation is the quickest way of solving that specific problem. This is even more the case if a higher number of quadrature points is used (as in Table I).

## V. Summary

We studied potential scattering without angular momentum decomposition in time-independent and time-dependent treatment. For higher energies the scattering amplitude may show a strong forward peak like in Fig. 1. This pronounced angular structure can easily be integrated in a Lippmann–Schwinger equation, whereas its presentation by partial waves is tedious as seen in Fig. 2. A direct use of the scattering angle as an integration variable in the integral equation should be even more profitable if spins are involved, like in a two-nucleon system, where already the partial-wave representation of the two-nucleon force in momentum space is quite involved [4]. An application for two nucleons interacting by OBE-potentials is underway.

The free propagator singularity in the Lippman–Schwinger equation can be avoided in a time-dependent treatment. The momentum space representation of the time-dependent wave function $\psi(t)$ during the interaction time is smoother than the configuration space representation. For large times $|t|$ when the particle is outside the range of the potential $f(\mathbf{q}, t) \equiv \langle \mathbf{q} \,|\psi(t)\rangle$ oscillates like $e^{-iE_q t}$ which is hard to control numerically. We proposed two ways to overcome that difficulty. For $t \to -\infty$ that oscillating factor occurs in the known initial momentum distribution $f_0(\mathbf{q}, t)$ and for $t \to -\infty$ in the unknown scattered part determined by the on-shell scattering amplitude. One parametrises the $q$-dependence of the scattered part by a

linear combination of test functions. Then the time evolution of the wave function can be followed form both sides, $t \to -\infty$ and $t \to +\infty$, till $t = 0$. Requiring the equality of the two solutions gained from both sides determines the on-shell scattering amplitude. Clearly not the time evolution of $f(\mathbf{q}, t)$ is handled numerically but of $f(\mathbf{q}, t)$ minus its oscillating asymptotic part.

In a second approach we tame the energy- and time-dependent oscillating factor by a contour deformation to complex momenta, see (III.29) and Fig. 4. Now we integrate from $t \to -\infty$ to $t \to \infty$ and regard the amplitude $R_t(\mathbf{q}, t) \equiv f(\mathbf{q}, t) - f_0(\mathbf{q}, t)$. The real part of $R_t(\mathbf{q}, t)$ is shown in Fig. 5 between $t = -10$ fm and $t = +15$ fm for complex momenta. One recognizes the strong damping for large times, which is in striking contrast to the strong oscillations of $R_t(\mathbf{q}, t)$ for real momenta and large times, shown in Fig. 6 Once $R_t$ for real momenta is determined by pure quadrature from $R_t$ depending on complex momenta the on-shell scattering amplitude can be easily extracted at large $t$-values It is also interesting to see in Figs. 7 and 8, how the angular structure of $R_t(\mathbf{q}, t)$ builds up in time with respect to the beam direction.

In the numerical treatment of the time evolution we split the total time interval into subintervals, in which the time dependence of $R_t$ is interpolated by polynomials. Then the time integration can be done analytically. It was very important to detect that by a suitable set of polynomials (in the most sophisticated case of this work cubic B-splines) the evolution kernel is the same for *all* intervals. Therefore, the additional time variable $t$ in a time-dependent treatment does not blow up the dimension of the problem unduly.

Both approaches, time-independent and time-dependent, work without angular momentum decomposition. They may be a valuable alternative to standard techniques.

## APPENDIX

We want to give a short introduction on how the B-splines can be used to calculate the $t'$-integral in (IV.1). For the underlying theory of the spline functions we refer to [5].

Consider the general problem of interpolating a function $f(t)$ at the points $t_i$ $(i = 1, ..., m)$ in the interval $[a, b]$ with

$$a \leqslant t_1 < t_2 < \quad \cdot < t_m \leqslant b \tag{A.1}$$

by means of a spline $S(t)$ of order $n$ (i.e., degree $n-1$ with $n \geqslant 1$):

$$\begin{aligned} S(t) &= \sum_{i=1}^{m} c_i N_{ni}(t) \qquad (a \leqslant t \leqslant b), \\ S(t_j) &= f(t_j) \qquad (j = 1, \ldots, m) \end{aligned} \tag{A.2}$$

The basis functions $N_{nl}$ may be defined with the help of divided differences in the following way. Let us first define the truncated power function

$$M_n(x,t) := (x-t)_+^{n-1} = \begin{cases} (x-t)^{n-1} & (x-t>0) \\ 0 & (\text{otherwise}) \end{cases} \tag{A.3}$$

(with $n \geq 1$) and its divided difference of order $k$ with respect to the variable $x$ (based on $x_{l-k}, x_{l-k+1}, \ldots, x_l$):

$$\begin{aligned} M_n[x_{l-k}, \ldots, x_l; t] &= \frac{M_n[x_{l-k+1}, \ldots, x_l; t] - M_n[x_{l-k}, \ldots, x_{l-1}; t]}{x_l - x_{l-k}} \\ M_n[x_l; t] &= M_n(x_l; t). \end{aligned} \tag{A.4}$$

Although it is not necessary to do so (see, e.g., [5]) we assume that all the points $x_1, \ldots, x_{m-n}$ (called "interior knots") do not coincide. With $2n$ additional knots ("exterior knots"; compare with [5])

$$\begin{aligned} x_{1-n} = x_{2-n} = \cdots = x_0 &= a \\ x_{m-n+1} = \cdots = x_{m-1} = x_m &= b \end{aligned} \tag{A.5}$$

we now make the following choice for the basis function $N_{nl}$ of the spline (called normalized B-splines):

$$\begin{aligned} N_{nl}(t) &= (x_l - x_{l-n})\, M_n[x_{l-n}, \ldots, x_l; t] \\ &= M_n[x_{l-n+1}, \ldots, x_l; t] - M_n[x_{l-n}, \ldots, x_{l-1}; t]. \end{aligned} \tag{A.6}$$

In the special case $n = 1$ one obtains from (A.3):

$$N_{1l}(t) = \begin{cases} 1 & (x_{l-1} \leq t < x_l), \\ 0 & (\text{otherwise}). \end{cases} \tag{A.7}$$

The following relations hold:

$$N_{nl}(t) \begin{cases} > 0 & (x_{l-n} < t < x_l), \\ = 0 & (t < x_{l-n} \text{ or } t > x_l), \end{cases} \tag{A.8}$$

$$N_{nl}(t) = \frac{t - x_{l-n}}{x_{l-1} - x_{l-n}} N_{n-1,l-1}(t) + \frac{x_l - t}{x_l - x_{l-n+1}} N_{n-1,l}(t). \tag{A.9}$$

With the help of (A.7) and (A.9) it is possible to compute the functions $N_{nl}(t)$ recursively.

Differentiation of $N_{nl}(t)$ yields

$$\dot{N}_{nl}(t) := \frac{d}{dt} N_{nl}(t) = \dot{M}_n[x_{l-n+1}, ..., x_l; t] - \dot{M}_n[x_{l-n}, ..., x_{l-1}; t]$$
$$= -(n-1)\{M_{n-1}[x_{l-n+1}, ..., x_l; t]$$
$$- M_{n-1}[x_{l-n}, ..., x_{l-1}; t].$$

This follows directly from the definition (A.4) and from

$$\dot{M}_n(x; t) = \frac{\partial}{\partial t} M_n(x; t) = -(n-1)(x-t)_+^{n-2} = -(n-1)\, M_{n-1}(t).$$

According to the definition (A.6) one therefore has

$$\dot{N}_{nl}(t) = (n-1)\left\{\frac{1}{x_{l-1} - x_{l-n}} N_{n-1,l-1}(t) - \frac{1}{x_l - x_{l-n+1}} N_{n-1,l}(t)\right\}. \tag{A.10}$$

This relation may be compared with (IV.14) in the case of interpolation by cubic polynomials!

We now take the definition (IV.16) and recursively calculate the integral

$$K_{nl}(z, x_0, t) := \int_{x_0}^{t} dt' e^{-z(t-t')} N_{nl}(t') \tag{A.11}$$

with $x_0 \leqslant t \leqslant x_m$.

Partial integration leads to

$$K_{nl}(z, x_0, t) = \frac{1}{z}\left\{e^{-z(t-t')} N_{nl}(t')\Big|_{x_0}^{t} - \int_{x_0}^{t} dt' e^{-z(t-t')} \dot{N}_{nl}(t')\right\}.$$

With the help of (A.10) one obtains the recurrence relation

$$K_{nl}(z, x_0, t) = \frac{1}{z}\left\{N_{nl}(t) - e^{-z(t-x_0)} N_{nl}(x_0)\right.$$
$$- \frac{n-1}{x_{l-1} - x_{l-n}} K_{n-1,l-1}(z, x_0, t)$$
$$\left. + \frac{n-1}{x_l - x_{l-n+1}} K_{n-1,l}(z, x_0, t)\right\}, \tag{A.12}$$

where in the trivial case ($n = 1$) we have

$$K_{1t}(z, x_0, t) = \int_{x_0}^{t} dt' e^{-z(t-t')} N_{1t}(t')$$

$$= \begin{cases} \frac{1}{z}\left[e^{-z(t-\hat{x}_t)} - e^{-z(t-\hat{x}_{t-1})}\right] & (x_{t-1} < t), \\ 0 \qquad \text{(otherwise)}, \end{cases} \tag{A.13}$$

with $\hat{x}_t := \min(x_t, t)$.

As in Section IV we find that the integrals $K_{nt}$ are invariant under a *uniform* translation of all knots and the variable $t$; i.e.,

$$\tilde{K}_{nt}(z, \tilde{x}_0, \tilde{t}) := \int_{\tilde{x}_0}^{\tilde{t}} d\tilde{t}'\, e^{-z(\tilde{t}-\tilde{t}')} \tilde{N}_{nt}(\tilde{t}')$$

$$= \int_{x_0}^{t} dt' e^{-z(t-t')} N_{nt}(t') = K_{nt}(z, x_0, t), \tag{A.14}$$

where

$$\tilde{t} = t + \Delta T, \qquad \tilde{t}' = t' + \Delta T,$$

$$\tilde{x}_i = x_i + \Delta T \qquad (i = 1-n, ..., m).$$

$\tilde{N}_{nt}$ = normalized B-splines of order $n$ based on the new set of knots $\{\tilde{x}_t\}$. The proof of (A.14) is based on the fact that the normalized B-splines $N_{nt}$ do not depend on the chosen set of knots; i.e,

$$\tilde{N}_{nt}(\tilde{t}) = \tilde{N}_{nt}(t + \Delta T) = N_{nt}(t), \tag{A.15}$$

provided that the new set of knots $\{\tilde{x}_t\}$ results from the old one $\{x_t\}$ by the uniform translation given above. This is immediately evident from the recurrence relation (A.9).

Let us return now to our concrete problem, i.e., the integral equation (IV.1). We want to interpolate the function $R_t(q, x, t)$ with respect to the variable $t$ in a given interval $a = T \leqslant t \leqslant T + \Delta T = b$ by a cubic B-spline ("cubic means that the *degree* of the spline is 3; i.e., we have a spline of *order* $n = 4$). The interpolation points $t_j$ are chosen in the form

$$t_j = T + (j-1)\frac{\Delta T}{m-1} \qquad (j = 1, ..., m) \tag{A.16}$$

and (for simplicity) we define the knots $x_l$ by

$$\begin{aligned} x_{-3} &= x_{-2} = x_{-1} = x_0 = T = t_1 \\ x_1 &= t_3 \\ &\vdots \\ x_{m-4} &= t_{m-2} \\ x_{m-3} &= x_{m-2} = x_{m-1} = x_m = T + \Delta T = t_m. \end{aligned} \tag{A.17}$$

In other words: with the exception of $t_2$ and $t_{m-1}$ all interpolation points coincide with a knot. This choice is just a practical one; many other definitions are possible, too.

We then put

$$\begin{aligned} R_l(q, x, t) &= \sum_{j=1}^{m} c_j(q, k)\, N_{4j}(t) \\ &= \sum_{j=k}^{k+3} c_j(q, k)\, N_{4j}(t) \end{aligned} \tag{A.18}$$

with $x_{k-1} \leqslant t < x_k$, where the last equal sign follows from (A.8).

With this ansatz and the definition (A.11) we go into the integral equation (IV.1):

$$\begin{aligned} \sum_{j=k}^{k+3} c_j(q, x)\, N_{4j}(t) = R_0^{(T)}(q, x, t) + \frac{1}{t} \sum_{j=1}^{k+3} K_{4j}(\iota E_q, T, t) \\ \times \int_C dq' q'^2 \int_{-1}^{+1} dx'\, v(q, q', x, x')\, c_j(q', x') \end{aligned} \tag{A.19}$$

($x_{k-1} \leqslant t < x_k$). We now discretize the integrals in $q'$ and $x'$ (as in (IV.7)) and obtain the system of linear equations:

$$\sum_{j=k}^{k+3} c_{j\alpha} N_{4j}(t_{\tilde{k}}) - \frac{1}{t} \sum_{j=1}^{k+3} K_{4j}(\iota E_{q_\alpha}, T, t_{\tilde{k}}) \sum_{\beta} V_{\alpha\beta} c_{j\beta} = R_{0\alpha}^{(T)}(t_{\tilde{k}}) \tag{A.20}$$

with $x_{k-1} \leqslant t_{\tilde{k}} < x_k$ ($\tilde{k} = 1, ..., m$ according to (A.16)).

Here we used the abbreviations

$$\begin{aligned} c_{j\alpha} &= c_j(q_\alpha, x_\alpha) \\ R_{0\alpha}^{(T)}(t_{\tilde{k}}) &= R_0^{(T)}(q_\alpha, x_\alpha, t_{\tilde{k}}). \end{aligned}$$

According to (A.14) and (A.15) the integral kernel in (A.20) does not depend on the respective time interval $[x_0, x_m] = [T, T + \Delta T]$ provided that all knots $\tilde{x}_j$ in the new interval have a fixed difference $\Delta T$ from the old ones (as in (A.14)). Thus the kernel has to be inverted just once in order to solve the system (A.20) with different right-hand sides $R_{0\alpha}^{(T)}(t_{\tilde{k}})$, i.e., in different time intervals.

## REFERENCES

1 A GOLDBERG, H SCHEY, AND J L SCHWARTZ, *Amer J Phys* **35**, 177 (1967), E A MCCULLOUGH AND R E WYATT, *J. Chem Phys.* **54**, 3578, 3592 (1971); K C. KULANDER, *J Chem Phys* **69**, 5064 (1978), K C KULANDER AND E J HELLER, *J Chem Phys.* **69**, 2439 (1978), J C GRAY, G A FRASER, D G TRUHLAR, AND K C KULANDER, *J Chem Phys* **73**, 5726 (1980), K C. KULANDER, *Nucl Phys A* **353**, 341c (1981)
2 L MÜLLER, University of Bochum preprint, 1983 (unpublished)
3 R A MALFLIET AND J A TJON, *Nucl Phys A* **127**, 161 (1969)
4 K ERKELENZ, *Phys Rep C* **13**, 191 (1974)
5 H B CURRY AND I J SCHOENBERG, *J Anal Math* **17**, 71 (1966); C DE BOOR, *J. Approx Theory* **6**, 50 (1972), M G COX, *J Inst Math Appl* **15**, 95 (1975)